*OLA 7.6.1 =Digest 3.1.*
*[Version 4 rev. 1 Aug 2013]*

**Tarbat Discovery Programme – Radiocarbon dating and Bayesian modelling**
by Derek Hamilton (SUERC)

Between 1992 and 2011, 72 radiocarbon measurements were produced from 71 samples representing 70 individual archaeological contexts from the Tarbat Discovery Programme. In total, the pool of samples comprised 36 on human bones, eight on charcoal, eight on charred grain, seven on wood, five on animal bone, four on the humic acids from bulk organic sediment, three on waterlogged seeds, and one on cremated animal bone.

Of the 71 samples, six samples (3 human bone and 3 bulk organic sediment) were submitted to the Scottish Universities Research and Reactor Centre, East Kilbride, and measured by liquid scintillation counting. The human bone was pretreated with a modified Longin (1971) method while the sediment was pretreated as described in Stenhouse and Baxter (1983), with the humic acid fraction reserved for dating. The samples were further processed and measured as described by Noakes et al. (1965). These results are identified by their GU- number.

Forty-eight samples were submitted to the Scottish Universities Environmental Research Centre, East Kilbride for Accelerator Mass Spectrometry dating (AMS). The 25 samples of human bone and five animal bone samples were pretreated using a modified Longin (1971) method. The 21 samples of charcoal and plant macrofossils were pretreated as described in Stenhouse and Baxter (1983). The sample of cremated animal bone was pretreated using the methods of Lanting et al. (2001). All the samples were combusted as described in Vandeputte et al. (1996), graphitized as described in Slota et al. (1987), and measured by AMS as described in Xu et al. (2004). These samples are identified by their SUERC- number.

The remaining samples were submitted to the Oxford Radiocarbon Accelerator Unit for AMS dating. The one sample of human bone was pretreated following the original 'ultrafiltration' method detailed in Bronk Ramsey et al. (2000), while the remaining 12 samples were pretreated using the improved 'ultrafiltration' method described in Bronk Ramsey et al. (2004a). The five samples of charcoal and wood were pretreated following methods described in Hedges et al. (1989). The samples were further processed and measured as described in Bronk Ramsey et al. (2004b). These are identified by their OxA- number.

Both laboratories maintain rigorous internal quality assurance procedures, and participation in international inter-comparisons (Scott 2003) indicate no laboratory offsets; thus validating the measurement precision quoted for the radiocarbon ages.

The radiocarbon results are given in Table 1 (*Digest 3.2*), and are quoted in accordance with the international standard known as the Trondheim convention (Stuiver and Kra 1986). They are conventional radiocarbon ages (Stuiver and Polach 1977).

The calibrations of the results, relating the radiocarbon measurements directly to calendar dates, are also given in Table 1. All have been calculated using the internationally agreed calibration curve of Reimer et al. (2009) and the computer program OxCal v4.1 (Bronk Ramsey 1995; 1998; 2001; 2009). The calibrated date ranges cited in the text are those for 95% confidence. They are quoted in the form recommended by Mook (1986), with the end points rounded outwards to 10 years if the error term is greater than or equal to 25 radiocarbon years or to 5 years if it is less. The ranges quoted in italics are posterior density estimates derived from mathematical modelling. The ranges in plain type in Table 1 have been calculated according to the maximum intercept method (Stuiver and Reimer 1986). All other ranges are derived from the probability method (Stuiver and Reimer 1993).

## Methodological Approach

A Bayesian approach has been adopted for the interpretation of the chronology (Buck *et al* 1996). Although the simple calibrated dates are accurate estimates of the dates of the samples, this is usually not what archaeologists really wish to know. It is the dates of the archaeological events represented by those samples, which are of interest. In the case of the Tarbat Discovery Programme, it is the chronology of the church and graveyard and that of the sequence of settlements beyond them that are under consideration. The dates of the overall chronological activity in each Sector can be estimated not only using the absolute dating information from the radiocarbon measurements on the samples, but also by using the stratigraphic relationships between samples.

Fortunately, methodology is now available which allows the combination of these different types of information explicitly, to produce realistic estimates of the dates of archaeological interest. It should be emphasised that the *posterior density estimates* produced by this modelling are not absolute. They are interpretative *estimates*, which can and will change as further data become available and as other researchers choose to model the existing data from different perspectives.

The technique used is a form of Markov Chain Monte Carlo sampling, and has been applied using the program OxCal v4.2. Details of the algorithms employed by this program are available from the on-line manual or in Bronk Ramsey (1995; 1998; 2001; 2009). The algorithm used in the model described below can be derived directly from the model structure shown in Figures 2–5.

## Stable Isotopes and Marine Correction

The C:N ratios for these samples suggest that bone preservation was sufficiently good to have confidence in the accuracy of the radiocarbon determinations (Table 1; Masters 1987; Tuross et al. 1988).

The $\delta^{13}C$ and $\delta^{15}N$ values from the majority of the earlier burials from this site (Fig 1) suggest a very small marine component in the diet, which is not likely to affect the radiocarbon dating significantly (Chisholm et al. 1982; Schoeninger et al. 1983). The same cannot be said for the later burials, nearly all of which have a moderate to significant marine signature.

When humans and non-human animals consume marine resources the radiocarbon age of their bones will be older than expected. The reason for this is that while the production and distribution of radiocarbon in the atmosphere is virtually instantaneous so that terrestrial plants and animals that feed on those plants will have their ratio of radiocarbon in equilibrium, when $^{14}C$ enters the oceans it does not become distributed instantaneously and 'hangs around' for awhile at some depth. The result is that the marine carbon cycle is not in sync with the terrestrial and marine ages are too old when calibrated with the terrestrial radiocarbon calibration curve.

It is possible to 'correct' radiocarbon ages for material whose protein has come from both terrestrial and marine sources (Bayliss et al. 2004). It should be stressed that this marine correction is, in essence, a modelled radiocarbon calibration that uses a mixture of the internationally agreed calibration curves IntCal09 and Marine09 of Reimer et al. (2009). It is a modelled calibration because there is more than one way to determine the percentage of diet that derived from terrestrial/marine resources. As such, the results will vary slightly depending on the method used.

The method employed here was to calculate the percentage of the diet that was terrestrial by using -12.5‰ and -20.0‰ as the end members for the $\delta^{13}C$, where -20.0‰ was the equivalent of 100% terrestrial and -12.5‰ was equal to 100% marine. The local marine reservoir correction (ΔR) of -29 ±51 was used (Russell 2011). Radiocarbon results with a marine component that was determined to be 1% or greater were corrected using OxCal and 'mixing' the two calibration curves at the calculated percentage. The corrected radiocarbon dates are given in Table 2, and these same corrected dates were used throughout the modelling of the results from Tarbat.

## The Tarbat Discovery Samples

Except for samples submitted from a palaeoenvironmental sequence (discussed below) all the samples were single-entities and from short-lived species (Ashmore 1999). The overall model employed combines the observed stratigraphy in the three excavated and dated sectors (Sectors 1, 2, and 4) with the samples discussed within their place in the overall site periodisation. While the samples are discussed below by period and then by sector, the model maintains independence between the dating of the individual sectors and uses the multiple estimations for period transitions across the sectors as a point for later discussion. Furthermore, the model only stipulates that the Periods are sequential, and that they are not necessarily temporally contiguous, which is attested to in some cases by the archaeology (e.g. wind-blown sand deposits at the transition from Period 1 and 2 in Sectors 2 and 4, and the burning event that marked the end of Period 2).

### *Period 1*

Seven features were dated from Sector 2 and placed into Period 1. There was no stratigraphy between these features. There is a result (SUERC-14989) from a bulk sample (C2310/4874) of waterlogged weed seeds from the marsh. SUERC-13277 is a result from a waterlogged willow stake in a pool (F436/C2224). SUERC-33420 is from a charred hazelnut shell recovered from a hearth (F535/C3406). SUERC-33421 is from a fragment of hazel woven to form the lining of a well (F527/C3570). SUERC-13263 is on a carbonized barley grain from the fill of a pre-church ditch (F129/C1345). There are two results (SUERC-13256 and -33416) on two burials (Burial 186/F515/C2987 and Burial 187/F516/C3346) that were excavated outside the church, but which form part of the cist burial cemetery that was excavated within the church. Finally, SUERC-14994 is on a fragment of waterlogged birch from a context (C2296/4873) which represents the end of the Period 1 peat deposits that were superseded by the pool in Period 2.

Six features, forming two sequences, in Sector 4 provided eight results. The first sequence of burials begins with Burial 170, a simple inhumation, with one result (SUERC-33413) on a rib, which is followed by another simple inhumation (Burial 169) from which there is a result (SUERC-33412) on a rib.

The second sequence begins with two results (SUERC-13255 and OxA-13483) from cist Burial 162. These two results are statistically consistent (T'=0.4; ν=1; T'(5%)=3.8: Ward and Wilson 1978) and have been combined prior to calibration to form **mean 162** (1546 ±21 BP). Burial 162 is stratigraphically coeval with Burial 172, from which there are two results (SUERC-37079 and OxA-9699) that are not statistically consistent at 2-sigma (T'=5.3; ν=1; T'(5%)=3.8: Ward and Wilson 1978), though they are at less than 3-sigma (T'(1%)=6.6). Given the two samples are from the same body, it is more likely that the measurements from the two labs are only slightly more variable than would usually be expected. The results have been combined prior to calibration to form **mean 172** (1441 ±23 BP). Burial 172 is followed

stratigraphically by cist Burial 146, which produced a single result (SUERC-37078) on a metatarsal. Burial 146 is of similar stratigraphic age to Burial 163 (they are not actually in contact), which produced a result (OxA-13484) on a leg bone from the probable shrouded inhumation.

*Period 2*

In Sector 1, there is one result (OxA-10159) from a wooden stake recovered *in situ* in the outer enclosure ditch. Three samples of bulked organic sediment taken from the early fill of the outer enclosure ditch in 1991 (Int 1) gave dates in the later Iron Age (GU-3265, -3266, and -3267). There is a result (SUERC-2621) on a fragment of cremated cattle bone recovered from the hearth (F65/C1141) in the Smith's Hall (S1), with a replicate measurement (SUERC-33415) made on a charred hazelnut shell from the same context. The two results are statistically consistent (T'=1.2; v=1; T'(5%)=3.8: Ward and Wilson 1978) and could be the same actual age.

There are 12 radiocarbon-dated contexts from Period 2 in Sector 2. A single date (SUERC-13581) is available from charred barley recovered the hearth (F495/C2786) in Structure 9. Four dates are available from features in the Structure 9 yard. SUERC-13272 is a result from a charred barley grain recovered from a hearth in the yard (F445/C2468). SUERC-13266 is from a cattle metatarsal recovered as part of a 'bone raft' beneath Structure 9 yard wall (F480/C3122). SUERC-13267 is from one of an alignment of worked cattle metapodials in the Structure 9 yard (F393/C1957), and this result is the earlier in a sequence with SUERC-13271, a result on a cattle metatarsal that was one in a cache of metapodials in the workshop yard (C2000). SUERC-13265 is on a cattle metatarsal from a horizon of butchered bone on the eastern roadside surface (C2335), and SUERC-13276 of a sample from a waterlogged willow stake that was recovered *in situ* in the nearby stream (F404/C2295).

The Period 2 sequence in Sector 2 ended with a widespread fire, providing a strong stratigraphic horizon in this sector. A burnt hazel stake from the terrace wall (F490/C2697) produced SUERC-13273, and OxA-9664 came from a sample of burnt structural timber from primary burning horizon [26/C1030]. These final two results were potentially in use for an extended period of time prior to the destruction level that they form a part of, and so the results are included here as providing a *terminus post quem* for that destruction. A Frisian sceat, originating in the Rhineland in AD 715-735 was redeposited in a pit of Period 3 (14-24/F185) and also provides a tpq for the fire. There is one result that relates directly to the date of the fire (SUERC-13274 and -13275) on burnt hazel wattles from the terrace wall that formed part of a primary burning horizon (F483/C2584 and C2704, respectively), while a bulk sample of waterlogged elder seeds in the latest pool deposit (C4863) produced SUERC-14995, which also marked the end of Period 2 in Sector 2.

There are nine burials that belong to Period 2 in Sector 4. The head support Burial 128 has a result (OxA-13487) on a humerus. Burial 165 provided a result (OxA-13509) from the tibia of this probable simple inhumation. The probable shrouded inhumation (Burial 160) provided a result (OxA-13486) on a leg bone. In addition to the previous three burials, there are three sequences of burials. There is a result (OxA-13488) on a humerus from a simple inhumation, Burial 144, which is followed by head support Burial 116, from which there is a result (OxA-13489) on a humerus. The second sequence begins with a result (SUERC-33414) from the rib of a simple inhumation (Burial 171), that is followed by Burial 130, from which there is a result (SUERC-33405) on a rib from a probable shrouded inhumation. The third sequence of burials begins with a result (SUERC-33404) on a rib bone from a shrouded inhumation (Burial 129), which is followed by a result (SUERC-33410) on a rib from shrouded inhumation Burial 153.

*Period 3*

In Sector 1 and 2, Period 3A represents the revival of activity and Period 3B a period of abandon.

*Period 3A*

In Sector 1 There are two results on single charred barley grains from oval Structure 5 features: SUERC-13283 is from the central pit (F13/C1027), and SUERC-13284 is from the ditch of the same structure (F3/C1153). These two dates relate to grain from the same structure and so should be contemporary, which would suggest the structure likely dates to the 9$^{th}$ or 10$^{th}$ century.

In Sector 2, SUERC-13281 is on a fragment of hazel charcoal from a metal-working hearth (F148/C1412) and represents the first stratigraphic event following the fire in Sector 2.

*Period 3B*

In Sector 1, SUERC-13285 is on a single charred barley grain recovered from the flue of the converted Structure 1 (F79/C1527) and should represent its last use. OxA-9662 is on a piece of unidentified charcoal that is part of the ultimate fill of the tributary ditch. SUERC-13286 is from a fragment of waterlogged willow that was in a deposit related to the early disuse of the enclosure ditch (F132/C1401). These events should be broadly contemporary.

In Sector 2, a pit that contained an articulated cow burial (F304/C1734) produced a result (SUERC-13282) from a metatarsal. This represents the final disuse of the road (S13).

There are three results from Period 3 burials in Sector 4. There is one result (OxA-13485) on the humerus from a possible wicker-lined burial (147). A second result (GU-9297) is available from the humerus of head support Burial 152, while the right humerus of shrouded inhumation Burial 158, provides the third result (GU-9296). From head support inhumation Burial 111, there is a result (SUERC-33402) on a rib. There are results from two bodies in a possible double-burial. From the first body (Burial 156) there is a result (SUERC-33411) on a rib, and from the second (Burial 136) there is a result (SUERC-33406) on a rib.

*Period 4*

The earliest dated events in Sector 4 (assigned to Period 4A) were a bell-casting pit (F107/C1220), which gave a result (OxA-10536) on a fragment of unidentified charcoal, and a single Burial 117, which gave a result (GU-9298) on a humerus. These are contemporary with the early church (Church 2).

There was single burial contemporary with the construction of Church 4 in Period 4B: Burial 110, from which there is a result (OxA-13490) on a juvenile tibia.

The main body of burials belong to a period after the refurbishment of Church 4 following a fire (Period 4C). The first is coffined Burial 112, from which there is a result (SUERC-33403) on a rib. There is a result (OxA-13941) from the tibia of a coffined, shrouded Burial 113, followed by another coffined, shrouded Burial 101 dated by a result (SUERC-33401) from a rib. Coffined Burial 90 produced result OxA-13521 on a humerus, while the shrouded Burial 98 produced a result (SUERC-33400) on a rib. Another shrouded inhumation (Burial 97) had a humerus dated (OxA-13762).

**Bayesian Modelling Results**

The model that follows the relationships given in the section above (Figure 2) has good agreement between the archaeology and the radiocarbon dates ($A_{model}$=67). The results for the start and end date of the major periods are given in Table 2, and Figures 3–6.

The chronological model for Sector 1 (Figure 3) begins with Period 2 and ends with a general Period 3. The model estimates that the potential hiatus between the two periods in this sector was *0–115 years* (*95% probability*; Fig 7; *Sector 1 Period 2/3 hiatus*), but maybe only up to *60 years* (*68% probability*).

The chronological model for Sector 2 (Figure 4) has a greater time-depth, beginning with Period 1 and continuing until Period 3B. Here the hiatus between Periods 1 and 2, as evidenced by the wind-blown sand deposit, was *0–95 years* (*95% probability*; Fig 7; *Sector 2 Period 1/2 hiatus*), and probably either *0–20 years* (*49% probability*) or *60–85 years* (*19% probability*). There was a break in activity between Periods 2 and 3, evidenced in Sector 2 by the site-wide fire that included the break up of sculpture with sledgehammers. The Period 2 and 3 are easily distinguishable and there is the possibility that there was another hiatus in activity at this time that lasted *0–210 years* (*95% probability*; Fig 7; *Sector 2 Period 2/3 hiatus*), and probably *5–150 years* (*68% probability*).

Sector 4 (Figure 5) has the greatest time-depth, and runs from Period 1 through Period 4. Here the hiatus between Periods 1 and 2 lasted *0–85 years* (*95% probability*; Fig 7; *Sector 4 Period 1/2 hiatus*), and probably for up to *55 years* (*68% probability*). The hiatus between Periods 2 and 3 lasted for *0–150 years* (*95% probability*; Fig 7; *Sector 4 Period 2/3 hiatus*), and probably for *1–90 years* (*68% probability*). The break between Periods 3 and 4 lasted for *0–160 years* (*95% probability*; Fig 7; *Sector 4 Period 3/4 hiatus*), and probably for *5–110 years* (*68% probability*).

It should be noted that based on the radiocarbon data alone, there is no clear evidence for a hiatus between any of the periods. The calculation of the difference between the end probability for one period and the start of the next always begins in the negative, which indicates the possibility for no hiatus. Given the archaeological evidence for hiatuses between periods in some sectors, it is worthwhile summarizing the data based on that evidence. The hiatus between Periods 1 and 2 was dated in Sectors 2 and 4, and suggested a break in activity on perhaps *one century* (*95% probability*), but perhaps only *a half-century* (*68% probability*). The estimated period for the break in activity following the widespread burning (Period 2 to 3) is more varied across the site and ranges from 1 to 2 centuries, but the consensus at *68% probability* is *between one-half and three-quarters of a century*. Any break in activity between Periods 3 and 4 would have probably lasted for *up to a century* (*68% probability*), though it might have lasted closer to a *century and a half* (*95% probability*).

**Table 3:** Probability ranges for the start and end dates of the different Periods, by Sector, derived from the modelling shown in Figures 3–5

| | **Sector 1 (Figure 3)** | **Sector 2 (Figure 4)** | **Sector 4 (Figure 5)** |
|---|---|---|---|
| *start: Period 1* | | *cal AD 525–650 (95%)* | *cal AD 420–600 (95%)* |
| | | *cal AD 570–635 (68%)* | *cal AD 500–580 (68%)* |
| *end: Period 1* | | *cal AD 635–730 (95%)* | *cal AD 645–725 (95%)* |
| | | *cal AD 645–685 (68%)* | *cal AD 655–690 (68%)* |
| *start: Period 2* | *cal AD 610–780 (95%)* | *cal AD 645–685 (50%) or cal AD 735–765 (45%)* | *cal AD 670–760 (95%)* |
| | *cal AD 670–745 (67%) or cal AD 760–770 (1%)* | *cal AD 655–675 (35%) or cal AD 745–760 (33%)* | *cal AD 675–715 (46%) or cal AD 730–750 (22%)* |
| *end: Period 2* | *cal AD 700–840 (95%)* | *cal AD 710–780 (95%)* | *cal AD 690–790 (95%)* |

| | | | |
|---|---|---|---|
| | *cal AD 725–800 (68%)* | *cal AD 710–725 (27%) or cal AD 750–770 (41%)* | *cal AD 705–725 (11%) or cal AD 745–780 (58%)* |
| *start: Period 3* | | *cal AD 735–965 (95%)* | *cal AD 720–895 (95%)* |
| | | *cal AD 765–840 (38%) or cal AD 850–910 (30%)* | *cal AD 770–855 (68%)* |
| *end: Period 3* | | | |
| | | | |
| *start: Period 3A* | *cal AD 740–880 (95%)* | | |
| | *cal AD 775–855 (68%)* | | |
| *end: Period 3B* | *cal AD 1025–1250 (95%)* | *cal AD 775–1130 (95%)* | *cal AD 1025–1175 (95%)* |
| | *cal AD 1035–1135 (68%)* | *cal AD 785–795 (2%) or cal AD 815–850 (7%) or cal AD 885–1015 (59%)* | *cal AD 1035–1120 (68%)* |
| *start: Period 4* | | | *cal AD 1085–1245 (95%)* |
| | | | *cal AD 1135–1215 (68%)* |
| *end: Period 4* | | | *cal AD 1470–1690 (95%)* |
| | | | *cal AD 1490–1590 (61%) or cal AD 1605–1625 (7%)* |

**Figure 1:** Plot of the stable isotope results for those human bone samples where there is both a $\delta^{13}C$ and $\delta^{15}N$ measurement available. The points plotted in blue are from earlier burials, while those in red are from the later burials. The boxes for the expected values of fully terrestrial versus fully marine values are based on the data of Mays (1998, fig 9)

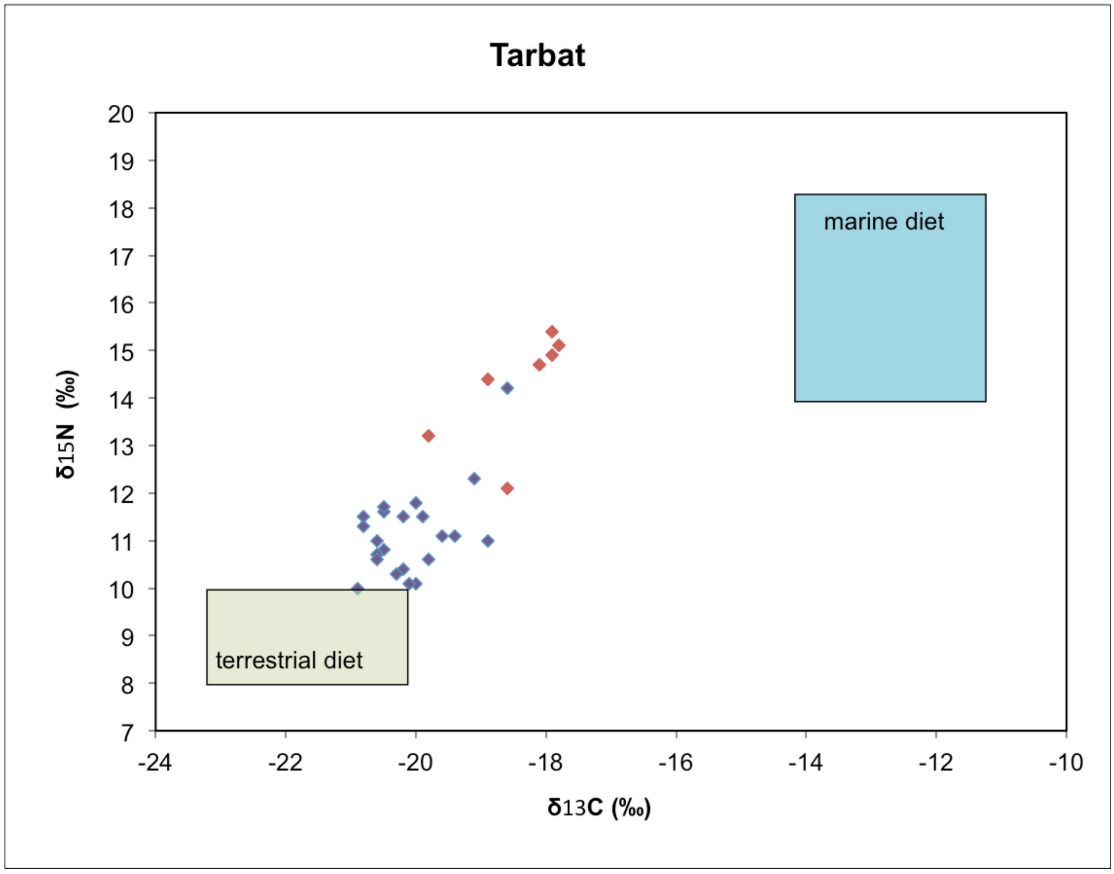

**Figure 2:** Simplified structure of the model for all three dated sectors at Tarbat.

**Figure 3:** Chronological model for the radiocarbon dates from Sector 1 at Tarbat. Each distribution represents the relative probability that an event occurred at some particular time. For each of the radiocarbon measurements two distributions have been plotted, one in outline, which is the result of simple radiocarbon calibration, and a solid one, which is based on the chronological model use. The other distributions correspond to aspects if the model. For example, '*start: Period 2 Sector 1*' is the estimated date that activity began at that site, based on the radiocarbon dating results. The large square 'brackets' along with the OxCal keywords define the overall model exactly

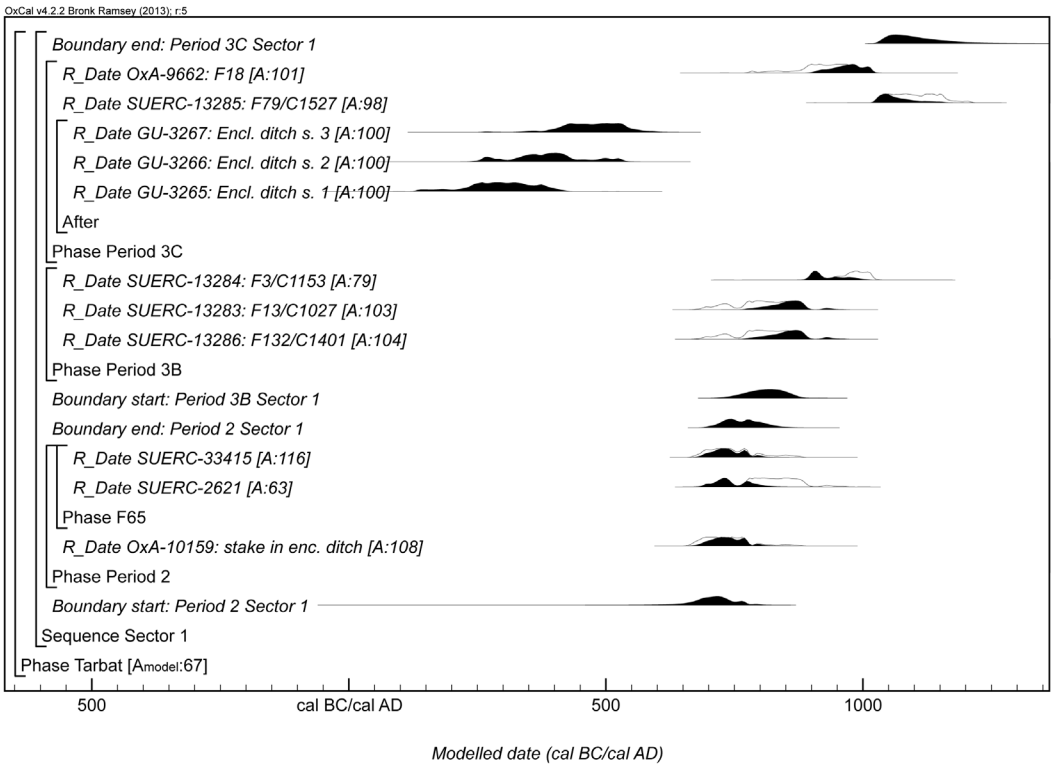

**Figure 4:** Chronological model for Sector 2 at Tarbat. The model structure is as described in Figure 3

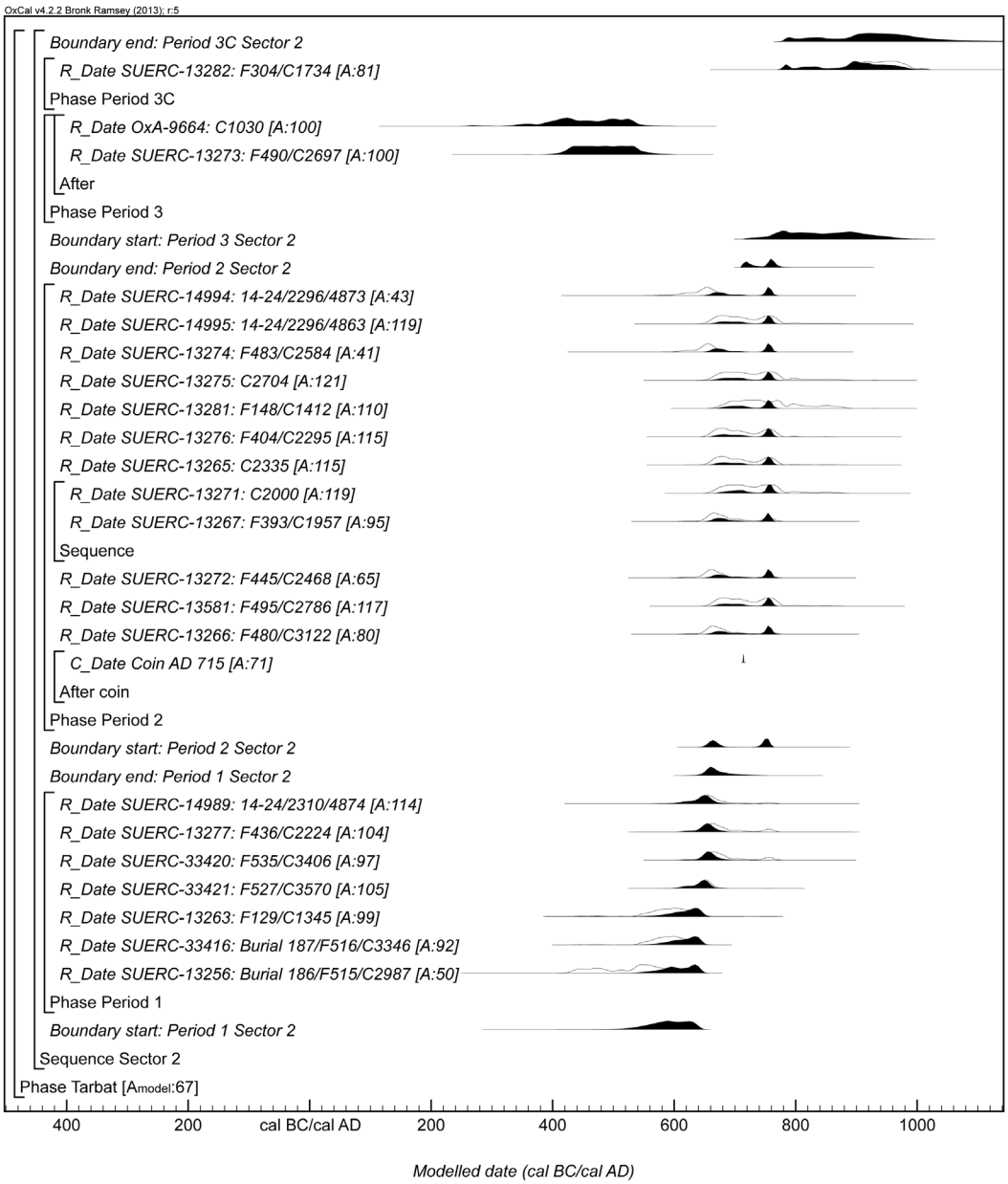

**Figure 5:** Chronological model for Sector 4 at Tarbat. The model structure is as described in Figure 3

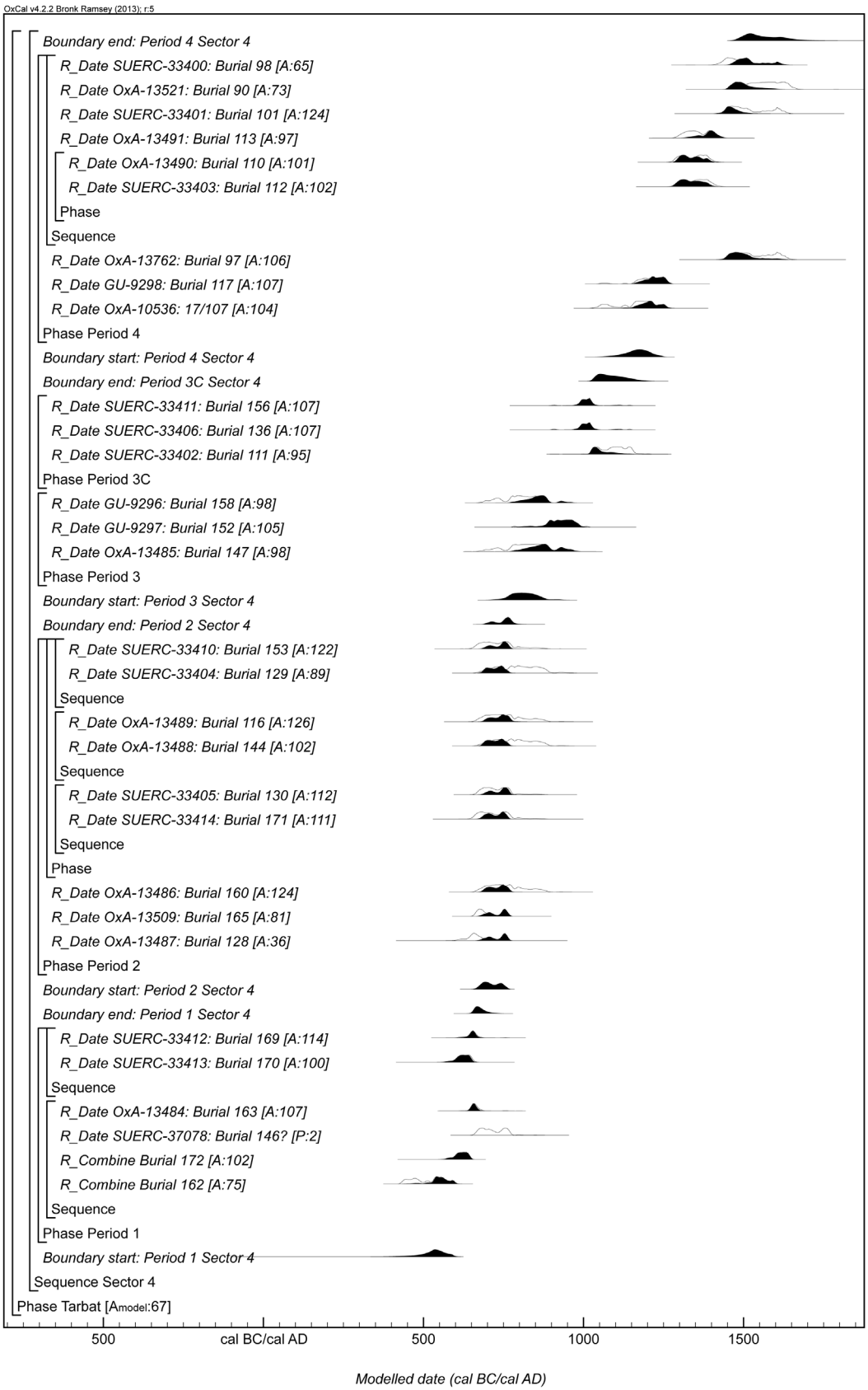

**Figure 6:** Summary of the transitions of all three sectors dated and modelled from Tarbat

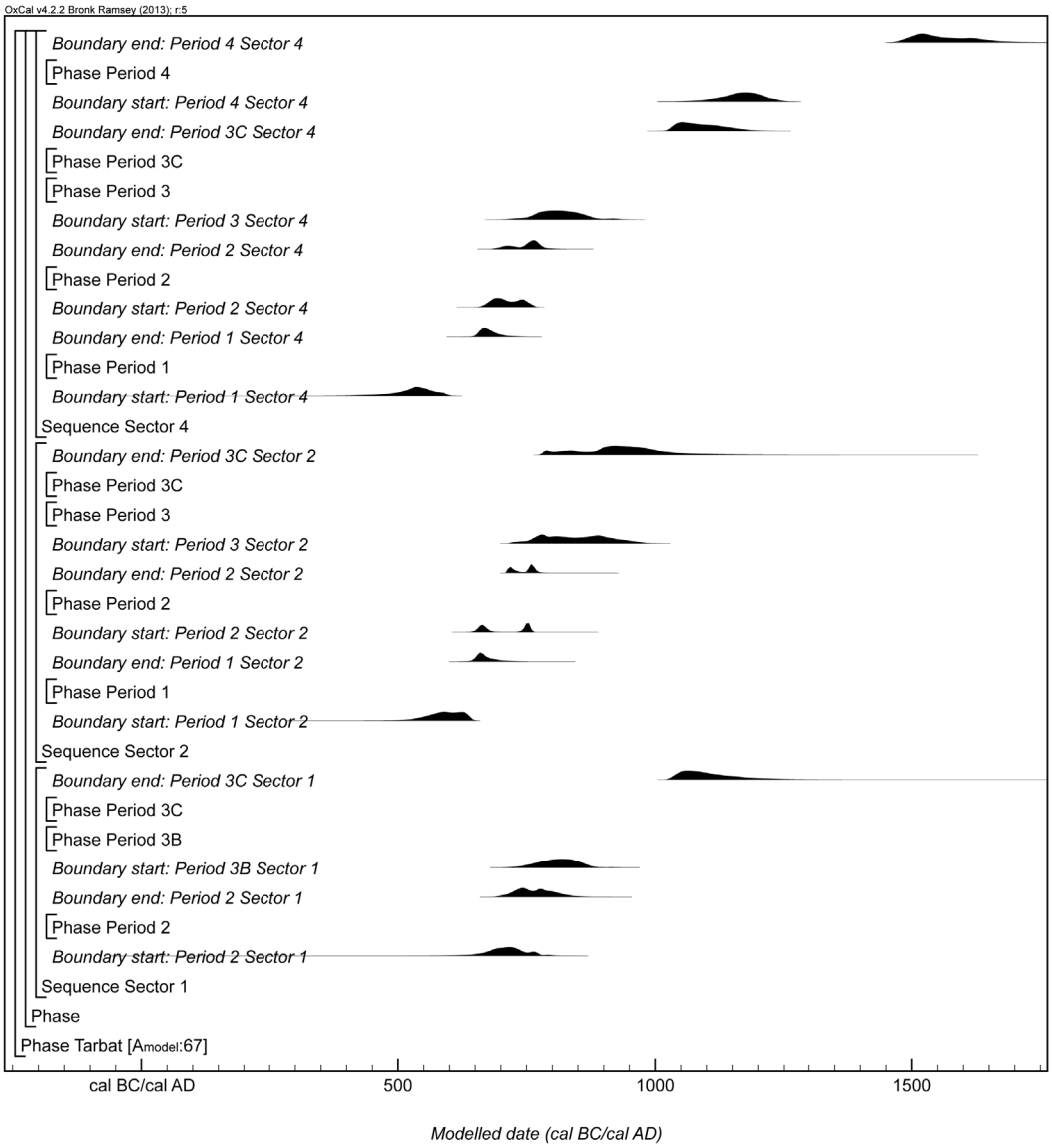


**Figure 7:** Ranges for hiatuses, and potential hiatuses, noted in the archaeology from Tarbat, calculated from the probability estimates shown in the models for Sectors 1, 2 and 4

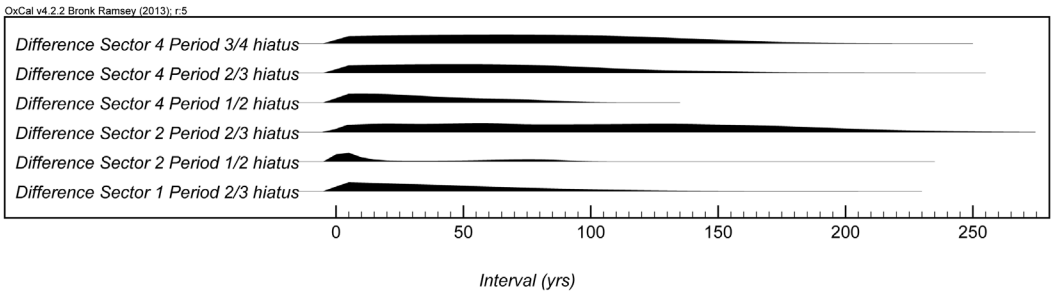

**Works Cited**

Ashmore, PJ 1999 Radiocarbon dating: avoiding errors by avoiding mixed samples, *Antiquity*, **73**(279), 124–30

Bayliss, A, Shepherd Popescu, E, Beavan-Athfield, N, Bronk Ramsey, C, Cook, GT, and Locker, A 2004 The potential significance of dietary offsets for the interpretation of radiocarbon dates: an archaeologically significant example from medieval Norwich, *Journal of Archaeological Science*, **31**, 563–75

Bronk Ramsey, C 1995 Radiocarbon calibration and analysis of stratigraphy: the OxCal program, *Radiocarbon*, **37**, 425–30

Bronk Ramsey, C 1998 Probability and dating, *Radiocarbon*, **40**(1), 461–74

Bronk Ramsey, C 2001 Development of the radiocarbon calibration program, *Radiocarbon*, **43**, 355–63

Bronk Ramsey, C 2009 Bayesian analysis of radiocarbon dates, *Radiocarbon*, **51**(1), 337–60

Bronk Ramsey, C, Pettitt, PB, Hedges, REM, Hodgins, GWL and Owen, DC 2000 Radiocarbon dates from the Oxford AMS system: Archaeometry datelist 30, *Archaeometry*, **42**(2), 459–79

Bronk Ramsey, C, Higham, T, Bowles, A, and Hedges, R 2004a Improvements to the pretreatment of bone at Oxford, *Radiocarbon*, **46**(1), 155–63

Bronk Ramsey, C, Higham, TFG, and Leach, P 2004b Towards high-precision AMS: progress and limitations, *Radiocarbon*, **46**(1), 17–24

Buck, CE, Cavanagh, WG, and Litton, CD 1996 *Bayesian approach to interpreting archaeological data*, Chichester: John Wiley & Sons, Ltd.

Chisholm, BS, Nelson, DE, and Schwarcz, HP, 1982 Stable carbon isotope ratios as a measure of marine versus terrestrial protein in ancient diets, *Science*, **216**, 1131–32

Hedges, REM, Law, IA, Bronk Ramsey, C, and Housley, RA 1989 The Oxford Accelerator Mass Spectrometry facility: technical developments in routine dating, *Archaeometry*, **31**, 99–113

Lanting, JN, Aerts-Bijma, AT, and van der Plicht, J 2001 Dating of cremated bone, *Radiocarbon*, **43**(2A), 249–54

Longin, R 1971 New method of collagen extraction for radiocarbon dating, *Nature*, **230**, 241–42

Mant, AK 1987 Knowledge acquired from post-War exhumations, in A Boddington, AN Garland, and RC Janaway (eds.) *Death, decay, and reconstruction*, Manchester: Manchester University Press, 65–80

Masters, PM, 1987 Preferential preservation of non-collagenous protein during bone diagenesis: implications for chronometric and stable isotope measurements, *Geochimica et Cosmochimica Acta*, **51**, 3209–14

Mays, S, 1998 *The archaeology of human bones*, London: Routledge

Mook, WG 1986 Business meeting: Recommendations/Resolutions adopted by the Twelfth International Radiocarbon Conference, *Radiocarbon*, **28**, 799

Noakes, JE, Kim, SM and Stipp, JJ 1965 Chemical and counting advances in Liquid Scintillation Age dating, in EA Olsson and RM Chatter (eds.), *Proceedings of the Sixth International Conference on Radiocarbon and Tritium Dating*, Pullman: Washington State University Press, 68–92

Reimer, PJ, Baillie, MGL, Bard, E, Bayliss, A, Beck, JW, Blackwell, PG, Bronk Ramsey, C, Buck, CE, Burr, GS, Edwards, RL, Friedrich, M, Grootes, PM, Guilderson, TP, Hajdas, I, Heaton, TJ, Hogg, AG, Hughen, KA, Kaiser, KF, Kromer, B, McCormac, FG, Manning, SW, Reimer, RW, Richards, DA, Southon, JR, Talamo, S, Turney, CSM, van der Plicht, J and Weyhenmeyer, CE 2009 INTCAL09 and MARINE09 radiocarbon age calibration curves, 0–50,000 years cal BP, *Radiocarbon*, **51**(4), 1111–50

Russell, N, 2011 *Marine radiocarbon reservoir effects (MRE) in archaeology: temporal and spatial changes through the Holocene within the UK coastal environment*, unpublished PhD thesis, University of Glasgow

Schoeninger, MJ, Deniro, MJ, and Tauber, H, 1983 Stable nitrogen isotope ratios of bone collagen reflect marine and terrestrial components of prehistoric diets, *Science*, **216**, 1381–3

Scott, EM 2003 The Third International Radiocarbon Intercomparison (TIRI) and the Fourth International Radiocarbon Intercomparison (FIRI) 1990–2002: results, analysis, and conclusions, *Radiocarbon*, **45**(2), 135–408

Slota Jr., PJ, Jull, AJT, Linick, TW and Toolin, LJ 1987 Preparation of small samples for $^{14}C$ accelerator targets by catalytic reduction of CO, *Radiocarbon*, **29**(2), 303–06

Stenhouse, MJ and Baxter, MS 1983 $^{14}C$ reproducibility: evidence from routine dating of archaeological samples, *PACT*, **8**, 147–61

Stuiver, M and Polach, HA 1977 Reporting of $^{14}C$ data, *Radiocarbon*, **19**(3), 355–63

Stuiver, M and Kra, RS 1986 Editorial comment, *Radiocarbon*, **28**(2B), ii

Stuiver, M and Reimer, PJ 1986 A computer program from radiocarbon age calibration, *Radiocarbon*, **28**, 1022-30

Stuiver, M and Reimer, PJ 1993 Extended $^{14}C$ data base and revised CALIB 3.0 $^{14}C$ calibration program, *Radiocarbon*, **35**(1), 215–30

Tuross, N, Fogel, ML, and Hare, PE, 1988 Variability in the preservation of the isotopic composition of collagen from fossil bone, *Geochimica et Cosmochimica Acta*, **52**, 929–35

Vandeputte, K, Moens, L and Dams, R 1996 Improved sealed-tube combustion of organic samples to $CO_2$ for stable isotope analysis, radiocarbon dating and percent carbon determinations, *Analytical Letters*, **29**(15), 2761–73

Ward, GK and Wilson, SR 1978 Procedures for comparing and combining radiocarbon age determinations: a critique, *Archaeometry*, **20**, 19–32

Xu, S, Anderson, R, Bryant, C, Cook, GT, Dougans, A, Freeman, S, Naysmith, P, Schnabel, C and Scott, EM 2004 Capabilities of the new SUERC 5MV AMS facility for $^{14}C$ dating, *Radiocarbon*, **46**(1), 59–64